A REDUCED ORDER MODEL TO PREDICT THE MACHINING TIME AND COST OF SMALL-SCALE RADIAL-INFLOW TURBINES

Matthias Geiselhart[1]*, Torben Anker Lenau[1], Jürg Schiffmann[2], Fredrik Haglind[1]

[1]Technical University of Denmark, Department of Mechanical Engineering
Nils Koppels Allé B403, 2800 Kongens Lyngby, Denmark

[2]École polytechnique fédérale de Lausanne, Laboratory for Applied Mechanical Design
Rue de la Maladière 71b, CP 526, 2002 Neuchâtel 2, Switzerland

*Corresponding Author: mgeis@mek.dtu.dk

ABSTRACT

This paper proposes a novel approach to predict the machining time of small-scale radial-inflow turbine impellers for organic Rankine cycle power systems based on preliminary design parameters. The time prediction method uses machining databases of different milling tools for the estimation of the cutting parameters, on which basis the flow channel volume and surfaces are discretized for the generation of preliminary milling toolpaths. The parameter selection comprises the material selection, the volume removed, the demanded surface quality and the tool selection governed by the accessibility due to geometrical limitations induced by the blades. The model is verified using computer-aided manufacturing software for two radial-inflow turbines cases: a state-of-the-art turbine using air and a turbine using the working fluid Novec 649 for a heat recovery application. The results highlight the governing role of the tool slenderness ratio on the actual manufacturing time. The relative time distribution among roughing, semi-finishing and finishing operations remain similar when considering the same production chain. The tool roughing strategy holds potential for optimization by contributing to approximately 60 % of the total milling time. Furthermore, the results indicate that the turbine manufacturing time can be improved by up to approximately 44 % when the maximum permissible load limits of the tools are exploited by customized cutting data. The presented machining time model can be applied in future works to predict the manufacturing costs of impellers and to quantify the influence of individual design features on the total cost by performing a sensitivity analysis. Moreover, the design space for optimal designs of small-scale radial-inflow turbines for organic Rankine power applications considering both the manufacturing time and the performance of the expander can be explored.

1 INTRODUCTION

The specific investment cost (SIC) of turboexpander increases with decreasing power output, causing unfavorable payback times for small-scale ORC power systems and calling for a deeper understanding of its manufacturing cost. Turbomachinery consist of rotationally symmetrical parts accommodating the electrical machine and parts characterized by their freeform shapes, namely nozzle, impeller and volute, which are exposed to the working fluid. The manufacturing effort for machined components, and thus their associated cost, increase with decreasing tool accessibility. Radial-inflow turbine impellers are characterized by their thin-walled freeform blades with undercut, which results in substantially higher manufacturing efforts. For low power applications and small batch sizes, 5-axis machine tools are commonly used. The integration of quantitative manufacturing parameters into the preliminary design stage, in which traditionally the thermodynamic efficiency is the main design target, can contribute to the achievement of a cost-effective solution. Methods to predict the manufacturing cost of such impeller designs are not available in the open literature.

Guillaume (2017) used the integrated cost estimation function of the computer-aided design (CAD) software suite Solidworks to suggest a cost function scalable with the impeller inlet diameter. Alternatively component manufacturers can be surveyed to identify empirical cost functions similar to Turton et al. (2018) or Astolfi et al. (2014). However, neither of these approaches enable to analyze the relationship between manufacturing effort and efficiency. Yet, design for manufacturability is a key aspect in the development of cost-effective turbomachinery components. In this respect, Chaves-Jacob et al. (2011) proposed a manufacturability indicator which represents qualitatively the difficulty to manufacture a certain turbomachinery impeller. Meroni et al. (2019) have recently linked the manufacturability indicator and turbine performance in a multi-objective optimization showing the interplay between ease of manufacturing and total-to-static efficiency of the turbine. Although different authors have addressed the cost issue to design and optimize RITs and ORC power systems, there are no previous works addressing the cost in a quantitative approach.

The time required to manufacture a workpiece is the factor governing its manufacturing costs. Thus, the manufacturing time is a suitable key figure to quantify the manufacturing expenses. According to Chang (2013), the manufacturing time can be obtained either by using a general approach based on the material removal rate, *MRR,* and surface generation rate, R_{sg}, or by carrying out virtual machining simulations. The general approach does not take into account the restricted accessibility of the machining area requiring the use of slender tools. Several computer-aided manufacturing (CAM) software suites provide functions for five-axis machining operations specifically designed for impeller machining. However, due to its industrial context, CAM workflows are custom made for each part and iterated until the part's geometrical requirements are met. The high computational effort of CAM software and the manual selection of tools and machining parameters hinder its automatization. Therefore, neither of these approaches are suitable for integration in the early turbine design phase.

This paper presents a novel approach to complement the preliminary design workflow of radial-inflow turbines (RIT), quantifying the manufacturing time with low additional computational effort. The machining process chain of a RIT design was modeled based on tool selection criteria and turbine design parameters provided by a 1D mean-line model. A scalable machining tool library based on publicly available tool data was coupled with a toolpath prediction method based on the discretization of volumes and surfaces according to geometric features of the tool and workpiece. The method was verified against the CAM manufacturing strategy of two radial-inflow turbines cases: a state-of-the-art turbine using air and a turbine using Novec 649 as working fluid for a waste heat recovery application.

2 METHODS

2.1 Cost modeling

According to Chang (2013), the unit cost of an in-house manufactured part, C_u, can be determined as

$$C_u = t_u \cdot (R_m + R_l) + C_{tool} + C_{mat} \tag{1}$$

with the unit time, t_u, the machining rate, R_m, the labor rate, R_l, the tooling cost, C_{tool}, and the material cost, C_{mat}. In the scope of this work the focus is put on the unit time, t_u, per impeller as the cost rates R_m and R_l are local production factors whereas the time can be used as target function for quantifying the optimization potential of the manufacturing strategies. The production time for one unit, t_u, is the sum

$$t_u = t_{su}/Q + t_o + t_{no} \tag{2}$$

of the setup time per unit, (t_{su}/Q), with the lot size, Q, operation time, t_o, and non-operation time, t_{no}. In the scope of this work, a model is presented to predict the operation time. The non-operation time and the setup time are not taken into consideration. The operation time for an impeller consists of the sum of the individual machining operations (Op) in the production chain

$$t_o = \sum (l_{c,Op} / v_{f,Op} + l_{a,Op} / v_{a,Op}) \tag{3}$$

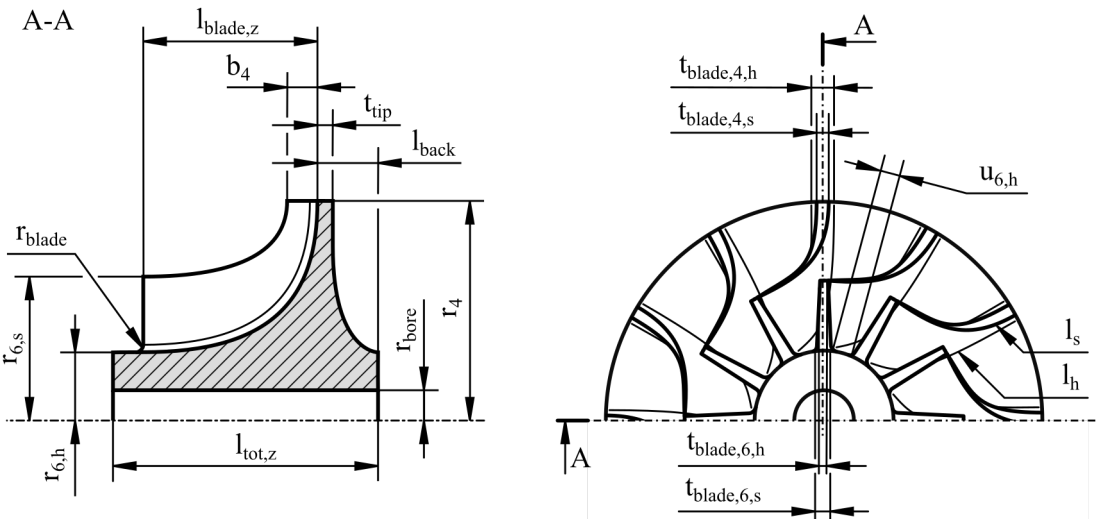

a) side section view b) top view

Figure 1: Schematic view and design variables of a radial-inflow turbine impeller

considering the duration lapsed from feed engagement to feed disengagement representing the tool path length, l_c, divided by the feed rate, v_f, and the tool travel distances, l_a, to approach the workpiece with free feed rate, v_a. The approach distance is negligibly small compared to the toolpath length with tool engagement and is therefore not taken into account.

2.2 Computer-Aided Manufacturing (CAM)

Computer-aided machining software applications use CAD geometry alongside machine, tool and stock definitions and user-specified parameters to generate a set of tool paths. In the scope of this work, the Mastercam software suite from CNC Software Inc. (2021) with the BladeExpert extension was used to analyze the manufacturing strategy. The analysis carried out in the CAM software consist of toolpath planning, residual material analysis, tool workspace restrictions and material under- or overcut due to the tool orientation.

2.3 Turbine design features

To begin the turbine design process with an accurate starting point, Mounier at al. (2018) proposed a new non-dimensional performance map tailored for small-scale turbines. The main dimensions of the blade were then calculated using the 1D mean-line model presented by Meroni et al. (2018). Based on the mean-line geometry, a preliminary three-dimensional design of the flow channel was generated according to the method proposed by Aungier (2006) to obtain the hub and shroud contours and blade curvatures. The turbine impeller design variables used to predict the machining time are illustrated in Figure 1 and complemented with the dimensions of the hub geometry. The availability of initial information about the three-dimensional geometry at the early design stage is key to estimate the manufacturing time of the turbine.

2.4 Case studies

Two case studies were used to assess the manufacturing time of the turbine impeller geometry. The first case study is a high-pressure ratio turbine operating with air and described by Jones (1996) and Sauret (2012). The second test case is an ORC turbine published by Meroni et al. (2019) using Novec 649 as working fluid. The required design parameters of the two turbine case studies using the mean-line model are listed in Table 1. The list is complemented with the required manufacturing parameters, which are up to the designer's choice. The stock material thickness for the semi-finish and finish operations were set to $t_{stock,sf} = 0.05$ mm and to $t_{stock,f} = 0.02$ mm, and the required surface roughness to $R_{a,sf} = 3.2$ µm and $R_{a,sf} = 3.2$ µm respectively. Stainless steel X14CrMoS17 was selected as a suitable workpiece material due to its good machinability and corrosion resistance.

Table 1: Geometrical features of a radial-inflow impeller linked to the machining strategy

Parameter		**Unit**	**Sauret (2012)**	**Meroni et al. (2019)**
Working fluid			Air	Novec 649
Power output	P	kW	121	6.55
Mean-line model Meroni et al. (2018)				
Number of blades	Z_r	-	16	14
Blade height at rotor inlet	b_4	mm	6.35	3.75
Impeller inlet radius	r_4	mm	58.1	35.4
Impeller outlet radius at shroud	$r_{6,s}$	mm	36.8	23.5
Impeller outlet radius at hub	$r_{6,h}$	mm	15.2	10.4
Impeller blade axial length	$l_{b,z}$	mm	38.9	19.6
Leading edge thickness at hub/ shroud	$t_{b,4,h} = t_{b,4,s}$	mm	1.01	0.75
Trailing edge thickness at hub/ shroud	$t_{b,6,h} = t_{b,6,s}$	mm	1.35	0.75
Fillet radius	r_{blade}	mm	1	1
3D model Aungier (2006)				
Impeller blade length at hub	l_h	mm	71.3	38.6
Impeller blade length at shroud	l_s	mm	53.6	32.6

2.5 Machining strategy

The aim of the machining operations is either to remove volume or to generate surfaces, referred to as roughing or finishing. The toolpath length, l_c, in Equation (3) is based on the length of each cutting sequence and the amount of sequences. The volumes and surfaces are discretized according to the tool's recommended machining parameters, in particular axial depth of cut, a_p, and radial depth of cut, a_e. The lengths of the impeller features are model for each machining operation. Starting from a cylindrical rough bar the production chain can be divided into two main stages: stage 1, lathing the contour and stage 2, milling of the blades. The subsequent rotor dynamic balancing is not taken into account.

Stage 1: Turning the contour

The strategy of the roughing operations is illustrated in Figure 2a. The aim is to remove the excess material around the outer contour while leaving a constant stock thickness along the contour for the subsequent finish operation. The described lathing process chain is performed in one single clamp. Errors caused by misalignment due to re-clamping in the lathing process chain are prevented, thus providing high concentricity of the outer contour and high perpendicularity of the planar backface with respect to the shaft seat axis.

Op 1.1: The material accessible in positive axial direction z is removed with V-shaped cutting inserts, shown in Figure 2a. This includes the planar front face, the elliptical backface contour and the reduction of the overall stock diameter, d_{stock}, to the inlet diameter, d_4.

Op 1.2: Drilling of the hole for the shaft seating with a slender drill bit shown in Figure 2d while the stock offers high rigidity.

Op 1.3: The shroud contour is cleared using a V-shaped lathe tool in opposite axial direction, as shown in Figure 2e. Thereby, the lathe chisel must create its free access space and forms a conical stock with a cone angle equivalent to the end cutting edge angle, Φ_a.

Op 1.4: The surface is finished by moving the V-shaped lathe tools along the outer contour as illustrated in Figure 2b. For improved stock stiffness conditions during finish operations, the outlet blade height b_6 is roughed from shroud outlet radius, $r_{6,shr}$, to hub outlet radius, $r_{6,hub}$, only after the surface finish is completed.

Op 1.5: The workpiece is separated from the stock bar with a tapping tool shown in Figure 2f.

The demanded surface roughness, R_a, is used to determine the feed rate, v_f. The tool tip radius, r_c, forms residual cusps on the lathed surface as shown in Figure 2b. The cusp width, w_{cusp}, is equivalent to the feed per revolution, f. The height of the cusp, h_{cusp}, is determined by the geometric relation between the cutter radius, r_c, and the cusp width, w_{cusp}:

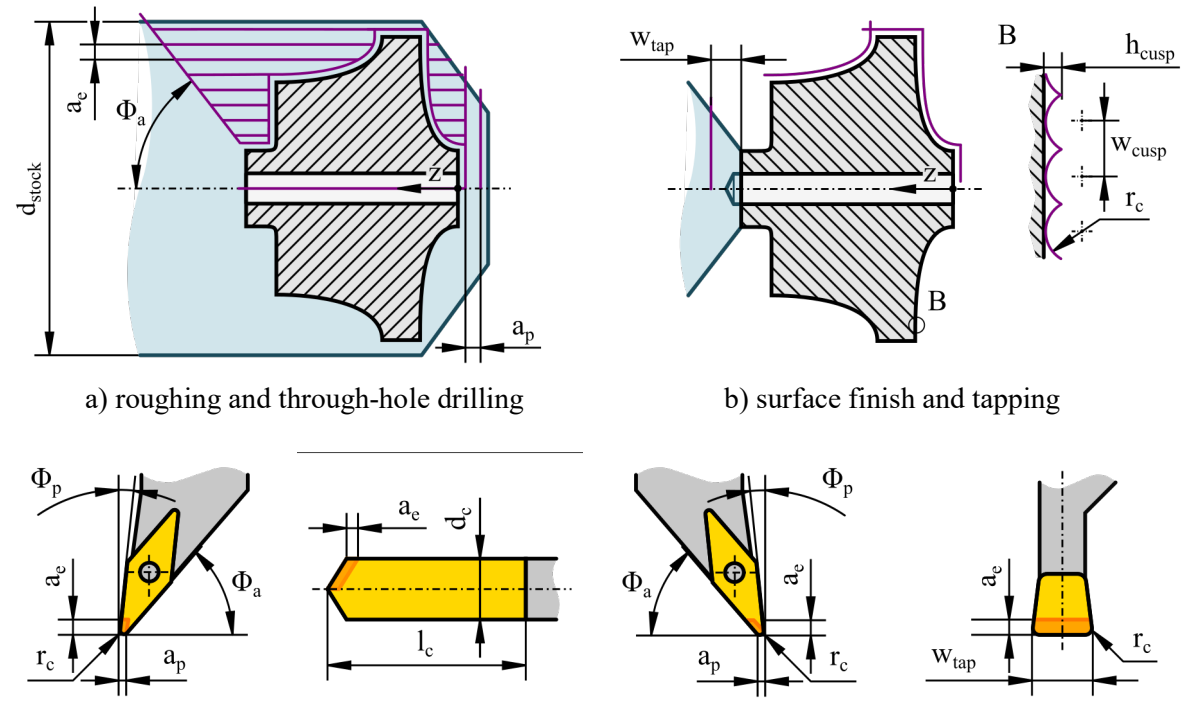

Figure 2: Schematic illustration of the lathing toolpath discretization of the outer contour based on the lathing tools used

$$h_{cusp} = r_c - \sqrt{r_c^2 - \frac{w_{cusp}^2}{4}} \approx R_t \approx 4R_a \tag{4}$$

Equation (4) is used as approximation to the peak-to-valley roughness R_t. and converted to the more commonly used arithmetic average roughness R_a by the factor 4 according to Qu and Shih (2003). It is generally accepted that the real values of the surface roughness deviate from the theoretical calculated values, primarily due to disturbance effects such as minimum chip thickness, deflections, vibrations or damages on the cutting edge. The presented model does not account for deviation caused by these sources of disturbance.

Stage 2: Milling of the blades

For the subsequent milling process chain, the impeller is clamped on the bore hole and backface geometry, keeping the alignment errors to a minimum.

Op 2.1: The screw seat front face is finished by removing residual material from the tapping operation with a bullnose end mill, shown in Figure 3c.
Op 2.2: Roughing the volume between the blades using one single bull nose tool, shown in Figure 3c, omitting the workpiece deflection by exploiting the rigid support of the stock material.
Op 2.3: Semi-finishing machining operations on the blade surface reduces the surface inequalities caused by the remaining roughing riblets. The freeform shapes of the hub and blade surface require the usage of ball nosed end mills for point milling, shown in Figure 3f.
Op 2.4: Semi-finish of the hub surface.
Op 2.5: Finish of the blade surface;
Op 2.6: Finish of the hub surface.

The freeform blades limit the accessibility for the solid milling cutters and thus add geometric complexity to the removal of the material between the blades. Furthermore, a constant stock material

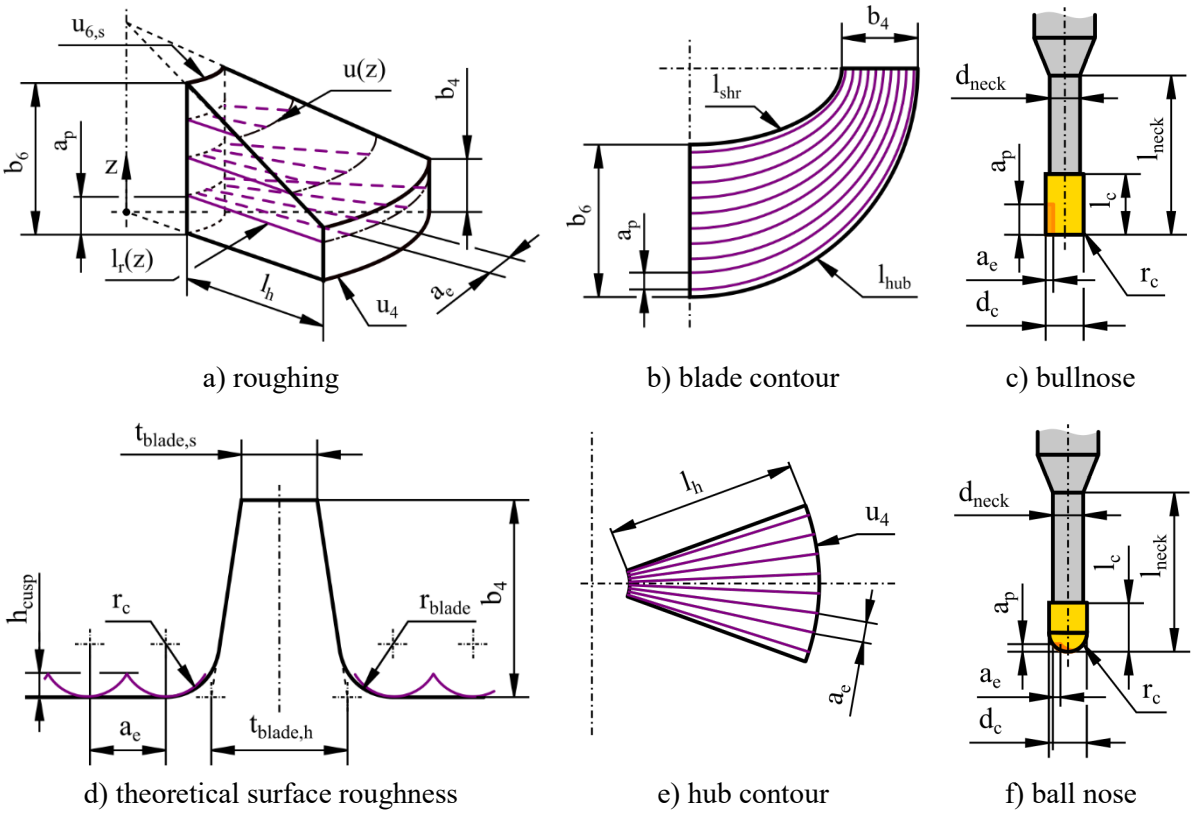

a) roughing b) blade contour c) bullnose

d) theoretical surface roughness e) hub contour f) ball nose

Figure 3: Schematic illustration of the milling toolpath discretization of the flow channel and blade surfaces based on the milling tools used

thickness, t_{stock}, is preferred to remain on the roughed surfaces to provide consistent milling conditions for the finishing operations. Constant cutter engagement conditions along the toolpath are crucial as the resulting cutting forces depend on the chip size removed per cut. Variations in chip load result in fluctuating cutting forces, causing workpiece and tool deflections. The resulting surface irregularities propagate from the roughing operations to the surface finishing operations. A key characteristic for the rigidity of milling tools is the tool slenderness ratio, R_{tool}

$$R_{tool} = l_{neck}/d_c \approx b_6/u_{6,h} \tag{5}$$

$$u_{6,h} = 2\pi \cdot r_{6,h}/Z_r - t_{b,6,h} - 2(t_{stock,sf} + t_{stock,f}) \tag{6}$$

between tool length, l_{neck}, and cutter diameter, d_c. According to Chaves-Jacob et al. (2011), R_{tool}, is recommended to be less than 4. However, the geometrical restrictions of the radial-inflow impeller imposed by the maximum blade height, b_6, and the minimum distance between two blades, $u_{6,h}$, require the selection of slender tools, hence violating this recommendation. The circumference at the outlet radius, $r_{6,h}$, is segmented by the number of blades, Z_r, and reduced by the blade thickness $t_{b,6,h}$. and by the remaining stock thickness for the semi-finish, $t_{stock,sf}$, and finish, $t_{stock,f}$, operation on both sides of the blade. In the scope of this work, the elastic tool and workpiece behavior is neglected. It is assumed that the cutting parameter recommendations sufficiently limit the tool loads below permissible thresholds.

The flow channel between two neighboring blades is described as a $1/Z_r$ section of a stacked cylinder and a truncated cone with a center hole, as illustrated in Figure 3a. To access the space in between the blades, the selected tool has to comply with Equation (5) and Equation (6). The number of milling layers is determined by fractioning the outlet blade height, b_6, by the axial depth of cut, a_p. The toolpath length, $l_r(z)$, is assumed as the radial length of the triangle spanned by the outlet edge and the cone surface and

is limited to the blade hub length, l_h. The amount of milling steps per layer is the fraction of the circumference of the circular segment, $u(z)$, by the radial depth of cut, a_e.

The ball end mills for semi-finish and finish operations require a longer neck length than the outlet blade height, $l_{neck} > b_6$. The fillet radius, r_{blade}, along the hub determines the milling diameter, $d_{c,sf}$, for semi-finishing.

$$d_{c,sf} = 2\,r_{blade} \tag{7}$$

The finishing tool requires a smaller cutter radius than the fillet radius to prevent scatter due to undefined cutter engagement conditions along the fillet and therefore is reduced by 0.1 mm. The same machining strategies are used for the semi-finish and finish operations. The toolpaths were generated by equally subdividing the hub and blade surfaces along the flow direction. As for the hub, all toolpaths have the same length as the blade edge on the hub, l_h, as illustrated in Figure 3e. In case of the blade, the toolpath length is interpolated between the hub and shroud edges as shown in Figure 3b. The number of toolpaths is determined by the specified surface roughness. The end mill forms residual cusps as shown in Figure 3d. The cusp width, w_{cusp}, in Equation (4), is equivalent to the cutter engagement in either radial, a_e, or axial, a_p, direction.

2.6 Machining parameters

The feed rate, v_f, used in Equation (3) is determined on the basis of machining parameter datasets for each individual tool of the manufacturing operations described in Section 2.5. The cutting parameter recommendations are provided by tool suppliers in tabular format and depend on the tool size, d_c, workpiece material and engagement conditions, a_p, and respectively, a_e. In the scope of this work, datasets from two different tool suppliers are used. The catalogue data from supplier (N), specialized in endmills with long neck length typically used in injection mold machining is applicable for a wide range of materials within on material class, stating conservative values. Supplier (S) provides an online accessible milling parameter calculator to obtain machining parameters tailored for a specific workpiece material and cutting engagement conditions, yielding optimized cutting conditions.

In case the tool selection is dependent on geometric features of the impeller, the feed rate is adapted according to the tool size and engagement conditions. The lathing tools are independent on geometric features due to the freely accessible outer contour of the impeller. The cutter tip radius, r_c, of the V-shaped insert is set to 0.8 mm, the width of the taping chisel, w_{tap}, to 4 mm and thus the feed rates of the chisels remain constant. The drill bit diameter is scaled with the impeller outlet radius at shroud, $d_c = r_{6,s}/2$ and its feet rate is adapted accordingly. For each milling operation a tool is automatically selected which complies with the geometric limitations of Equation (6) and Equation (7). The proposed model linearly interpolates the tabular data according to the geometric conditions of the individual tool.

3 RESULTS AND DISCUSSION

The CAM simulations for lathing the contour in Op 1.1 - 1.5 yield 4m:38s of total operation time for the air impeller and 2m:48s for the Novec impeller. Compared to 7h:55m:28s for milling one blade of the air and 25m:32s for the Novec blade with Op 2.1 - 2.6, the total time needed to accomplish stage 1 has a negligible impact on the overall machining time and was therefore not taken into account in the model. In contrast to the undercut volume in between two blades in stage 2, the outer contour is accessible without geometric limitations. Thus, rigid lathe tools are used with high material removal rates. Same applies for the front face milling operation Op 2.1.

Figure 4 shows the toolpath length and the machining time of one blade of the two turbine cases. The air impeller with a tool slenderness ratio, R_{tool}, of 6.9 compared to the Novec turbine with 4.6 can only be accessed using tools from supplier (N). The Novec impeller was analyzed with both machining parameter sets (N) and (S). As basis for the time prediction calculation, the predicted tool path lengths show good agreement with the toolpath lengths from the CAM simulation for all modeled machining

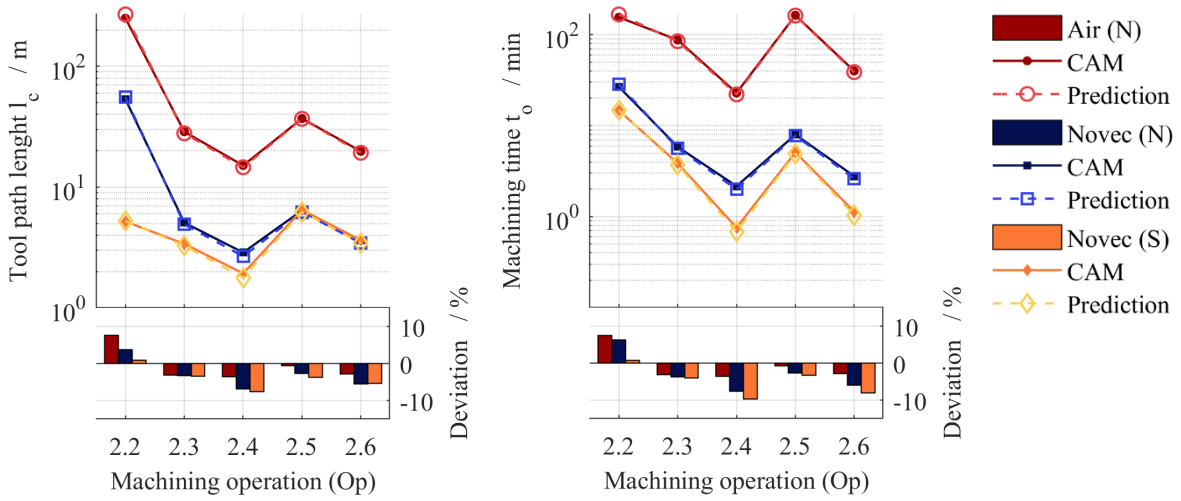

a) milling tool path length b) milling time

Figure 4: Comparison of predicted and simulated toolpath lengths and machining time per blade for the investigated RIT impeller geometries

operations with a maximum deviation of less than 8 %. The applied roughing strategy in Op 2.2 using one single tool results into the longest toolpath, as the flow channel volume is discretized with small cutter engagement. The overprediction for the roughing operation Op 2.2 is due to the fillet radius at the hub, which furthermore reduces the distance between the blades. Therefore, not all depths in the narrowest hub areas can be machined in the CAM simulation The milling operations with ball nose end mills are underpredicted, showing larger deviations for the hub operations Op 2.4 and Op 2.6 than for the associated blade milling operations Op 2.3 and Op 2.5. The milling step width, w_{cusp}, according to Equation (4), is the same for both semi-finishing operations Op 2.3 and Op 2.4 using the same tool. The two finishing operations Op 2.5 and Op 2.6 use a 0.1 mm smaller cutter diameter, resulting in a reduced milling step width, w_{cusp}. A relatively lower number of passes due to the deduction of the milling diameter, d_c, from the circumferential inlet edge length, u_4, lead to higher deviations for the hub milling operations. The machine time was calculated by dividing the toolpath length, l_c, by the feed rate, v_f. The predicted machining times show good agreement with the actual machining times from the CAM simulation for all machining operations. The deviation is less than 10%.

When the slenderness tool ratio of the tool increases, the overall manufacturing time increases. Figure 5 depicts the breakdown of machining time for the three turbine cases. The results indicate that the total milling time, t_{tot}, decreases with either (a) lower tool slenderness ratio, R_{tool}, or (b) customized cutting parameters. Optimized cutting parameters are independent on geometric features, therefore, the slenderness of the tool is the governing optimization parameter with respect to design for manufacturing. The cutting force is proportional to the chip removed. To achieve the demanded level of accuracy, the cutting force is limited by the permissible deflection of the tool. Therefore, an increase in the neck length results in a reduction of the chip load. This is highlighted by the customized cutting parameters from supplier (S), where the permissible cutting force limits are exploited to a larger degree for the given machining conditions. A comparison of the results shown in Figure 5b and Figure 5c indicates a time reduction by 44%. Catalogue data as provided by supplier (N) state conservative cutting parameters instead. The custom cutting recommendations for the bullnose cutter in Op 2.2 lead to a significant reduction of the roughing toolpath length by a factor 10 but do not over proportionally reduce the roughing time compared to the point milling operations. The large tool engagement is compensated by a reduced feed rate but results in higher step size residuals causing unsteady and therefore unfavorable cutter engagement conditions during the subsequent point milling operations. The proportions of the hub and blade milling operations differ not only in the double travel length per segment but also in the orientation of the ball nose end mill to the workpiece. The tool is oriented almost

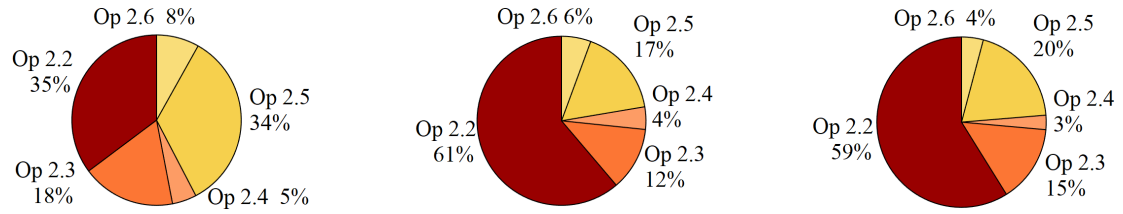

a) Air (N); t_{tot} = 7h:55m:28s b) Novec (N); t_{tot} = 0h:45m:31s c) Novec (S); t_{tot} = 0h:25m:32s

Figure 5: Breakdown of the machining time per milling operation for one blade

normal towards the hub where it is cutting with the tip of the sphere resulting in a smaller effective cutter diameter with higher feed rates. During the blade milling operation, the ball end mill is oriented almost parallel to the surface, cutting with the nominal cutter diameter. To keep the cutting speed, v_c, constant at the cutting edge, the feed rate is reduced. As the machining process chain and strategy was not changed in the scope of this study, further time reduction can be achieved by (a) improved roughing strategies, (b) neglecting the semi-finishing operations, or (c) using flank mills for the blade milling operations.

Processing the toolpath code in the CAM validation tool took 4:52 minutes for the air impeller and 1:07 minutes for the Novec impeller excluding the time for setting up the geometry and tool properties. The difference in computational time is due to the substantially longer toolpath and thus higher amount of numerical control (NC) code lines for the air impeller. The presented model took 0.85 seconds of computational time for the air impeller and 1.08 seconds for the Novec impeller and therefore can be integrated into a design optimization.

4 CONCLUSIONS

This paper presented a novel approach to predict the machining time for radial-inflow turbine impellers at the preliminary design stage without the use of computer-aided engineering software. The time prediction method uses machining databases of different milling tools for the estimation of the feed rate and engagement conditions, on which basis the flow channel volume and surfaces are discretized for the generation of preliminary milling toolpaths. The method was verified against results from computer-aided manufacturing software for the design of two turbine test cases. Tool catalog data and customized cutting recommendations were used as databases. The results of the two turbine designs highlight the governing role of the tool slenderness ratio on the actual manufacturing time. The results indicate that the relative time distribution among roughing, semi-finishing and finishing operations remain similar when considering the same production chain. The single tool roughing strategy omits deflection of the workpiece providing improved starting conditions for the subsequent ball nose milling processes for the hub and blade surfaces but at the expenses of approximately 60% of the total milling time. Furthermore, the results indicate that the turbine manufacturing time can be reduced by up to approximately 44 % when the tools maximum permissible load limit of the is exploited by customized cutting data. The method and results presented in this work reveal manufacturing limits and cost reduction potentials towards the development of cost-effective radial-inflow turbines. The low computational effort of the model and the reduced order of geometric data input required enables the integration of detailed machining time estimations into any design stage of a turbine. Future work includes to perform design optimizations of radial-inflow turbines considering both, the turbine performance and manufacturing efforts.

NOMENCLATURE

a_e	radial cutter engagement	(m)	l	length	(m)

a_p	axial cutter engagement	(m)	r	radius	(m)
b	blade height	(m)	R	ratio	(–)
C	cost	(EUR)	t	time	(sec)
d	diameter	(m)	t	thickness	(m)
f	feed per revolution	(m/rev)	u	circumference segment	(m)
f_z	feed per tooth	(m/tooth)	v_f	feed rate	(m/min)
h	height	(m)	Z_r	number of blades	(–)

Subscript

4	rotor inlet	b	blade	h	hub	sf	semi-finish
6	rotor outlet	c	cutter	r	roughing	tot	total
av	average	f	finish	s	shroud	z	axial direction

Abbreviations

CAD	computer-aided design	ORC	organic Rankine cycle	
CAM	computer-aided manufacturing	RIT	radial-inflow turbine	
Op	manufacturing operation	SIC	specific investment cost	(EUR/kW)

REFERENCES

Astolfi, M., Romano M. C., Bombarda P., Macchi, E., 2014, *Binary ORC (Organic Rankine Cycles) Power Plants for the Exploitation of Medium-Low Temperature Geothermal Sources* - Part B: Techno-Economic Optimization, *Energy*, no 66: p. 435–446.

Aungier, R. H., 2006, *Turbine Aerodynamics: Axial-Flow and Radial-Inflow Turbine Design and Analysis*. ASME Press, p. 233-263.

Chang, K. H., 2013, *Product Manufacturing and Cost Estimating Using CAD/CAE*, Elsevier, Oxford, p. 239-291.

Chaves-Jacob, J., Poulachon G., Duc E., and Geffroy C., 2011, Design for Manufacturing Applied to Turbomachine Components, *Int J Adv Manuf Technol*, vol 57, p. 453–463.

CNC Software Inc. 2021, Mastercam 2021 Update 3, www.mastercam.com.

Guillaume, L., 2017, On the Design of Waste Heat Recovery Organic Rankine Cycle Systems for Engines of Longhaul Trucks, PhD thesis, University of Liege.

Jones, A., 1996, Design and Test of a Small, High Pressure Ratio Radial Turbine, Journal of Turbomachinery, vol. 118, no. 2, p. 362–370.

Meroni, A., Geiselhart, M., Ba, W., and Haglind, F., 2019, Preliminary Design of Radial-Inflow Turbines for Organic Rankine Cycle Power Systems Considering Performance and Manufacturability Aspects, *5th International Seminar on ORC Power Systems - Athens, Greece*,

Meroni, A., Robertson, M., Martinez-Botas, R., Haglind, F., 2018, A Methodology for the Preliminary Design and Performance Prediction of High-Pressure Ratio Radial-Inflow Turbines, *Energy*, vol. 164, p. 1062–78.

Mounier, V., Olmedo, L. E., Schiffmann, J., 2018, Small Scale Radial Inflow Turbine Performance and Pre-Design Maps for Organic Rankine Cycles, *Energy*, vol. 143, p.1072–1084.

Qu, J., Shih, A. J., 2003, Analytical Surface Roughness Parameters of a Theoretical Profile Consisting of Elliptical Arcs, *Machining Science and Technology,* vol. 7, no. 2, p. 281–294.

Sauret, E., 2012, Open Design of High Pressure Ratio Radial-Inflow Turbine for Academic Validation, *ASME International Mechanical Engineering Congress and Exposition, Proceedings (IMECE)*, vol. 7, p. 3183–97

Turton, R., Shaeiwitz J.A., Bhattacharyya D., 2018, *Analysis, Synthesis, and Design of Chemical Processes*, 5th ed., Prentice Hall.

ACKNOWLEDGEMENT

The research was partly developed within the project “Clean Shipping on Green Fuel” (18-M10-DTU), funded by the Ministry of Foreign Affairs of Denmark and administrated by Danida Fellowship Centre.